

**MODAL ANALYSIS OF EMBEDDED PASSIVE DAMPING  
MATERIALS IN COMPOSITE PLATES WITH DIFFERENT  
ORIENTATIONS**

**Final Report  
For  
NASA – Dryden Flight Research Center  
Joint Research Interchange  
May 1, 1997 – July 24, 1998**

**Micheal Kehoe, Chief  
Aero. Structure Branch  
NASA – Dryden Flight Research Center**

**Faysal A. Kolkailah, Ph.D., P.E.,  
Principal Investigator  
Eltahry I. Elghandour, Ph.D.,  
Co-Principal Investigator  
Aeronautical Engineering  
California Polytechnic State University**

Funds for the support of this study have been allocated by the NASA – Dryden Research Center, Moffett Field, California, under interchange No. NAG4-138

## Abstract

This report presents an experimental and numerical investigation of the free vibration of cantilevered composite plates with and without passive damping. A total of seven composite material plates are considered. The lay-up sequences for the two plates without damping are  $[90/90/0/0]_s$  and  $[90/0/90/0]_s$ ; the other five plates are the same as the first two with two embedded layers of passive damping material. The passive damping material is embedded at different locations in the plate with orientation  $[90/0/90/0]_s$ . The damping material employed is a 3M material (SJ-2015 ISD 112) with peak damping properties in the ambient temperature range (32°F to 140°F). The composite material used is a carbon fiber (977-2)/epoxy resin (IM7). The effect of the passive damping system employed in this study for the composite plates are discussed. Modal testing is performed on these plates to determine resonant frequencies, amplitude and mode shape information. Numerical results are obtained using COSMOS/M software for the plates without damping. The experimental and numerical results are in very good agreement for different laminated plates without damping layers.

## **Acknowledgements**

We would like to thank NASA Dryden Flight Research Center for their sponsorship of this study. In addition, we would like to take this opportunity to express our gratitude to Mike Kehoe for his technical and administrative assistance during the course of this research effort and many others in the past. Last, but certainly not least, we would like to thank our Ph.D. student Khaled A. Alsweify and MSc. Student Cecilia Booker for their assistance in this project.

## Table of Contents

	<b>Page</b>
<b>Abstract</b>	<b>2</b>
<b>Acknowledgments</b>	<b>3</b>
<b>List of Tables</b>	<b>5</b>
<b>List of Figures</b>	<b>6</b>
<b>Nomenclature</b>	<b>7</b>
<b>Introduction</b>	<b>8</b>
<b>Objective</b>	<b>9</b>
<b>Experimental Procedure</b>	<b>10</b>
<b>Fabrication of Composite Plates</b>	<b>10</b>
<b>Identifying Resonant Node Lines</b>	<b>13</b>
<b>Dynamic Testing</b>	<b>13</b>
<b>Chirp Signal Tests</b>	<b>14</b>
<b>Results and Discussion</b>	<b>16</b>
<b>Expeimental Results</b>	<b>16</b>
<b>Numerical Results</b>	<b>24</b>
<b>Conclusion</b>	<b>27</b>
<b>References</b>	<b>28</b>

## List of Tables

Table 1. Material properties for 977-2 carbon fiber/ IM7epoxy resin	10
Table 2. Material properties for 3M viscoelastic damping layer, SJ2015 type 1205	10
Table 3. Plate dimensions and sequence with and without damping material	12
Table 4. Equipment and Instrumentation Summary	14
Table 5. Frequency modes for different orientations with and without embedded layers	22
Table 6. Numerical and experimental resonant frequencies for plates without damping	24

## List of Figures

Figure 1.	Composite material plate with embedded damping layer	11
Figure 2.	Cantilever Plate	12
Figure 3.	Schematic of Dynamic Testing	13
Figure 4.	Frequency response of chirp excitation for different orientations without damping	17
Figure 5.	Voltage of sensor output vs. time through transition from undamped to damped system for $[90/0/90/0]_s$ and $[90/90/0/0]_s$	17
Figure 6.	Frequency response of chirp excitation for orientations $[90/90/0/0]_s$ and $[90/90/0/0/d]_s$	18
Figure 7.	Voltage of sensor output vs. time through transition from undamped to damped system for $[90/90/0/0]_s$ and $[90/90/0/0/d]_s$	18
Figure 8.	Frequency response of chirp excitation for orientations $[90/0/90/0]_s$ and $[90/0/90/0/d]_s$	19
Figure 9.	Voltage of sensor output vs. time through transition from undamped to damped system for $[90/0/90/0]_s$ and $[90/0/90/0/d]_s$	19
Figure 10.	Frequency response of chirp excitation for orientations $[90/90/0/0/d]_s$ and $[90/0/90/0/d]_s$	20
Figure 11.	Voltage of sensor output vs. time through transition from undamped to damped system for $[90/90/0/0/d]_s$ and $[90/0/90/0/d]_s$	20
Figure 12.	Frequency response of chirp excitation for orientation $[90/0/90/0]_s$ with and without damping embedded at different locations	21
Figure 13.	Voltage of sensor output vs. time through transition from undamped to damped system for orientation $[90/0/90/0]_s$ with and without damping	21
Figure 14.	Voltage of sensor output vs. time through transition from undamped to damped system for orientation $[90/0/90/0]_s$ with damping	23
Figure 15.	Finite element modal and mode shape of plate A, $[90/90/0/0]_s$	25
Figure 16.	Finite element modal and mode shape of plate A, $[90/0/90/0]_s$	26

## Nomenclature

Plate A	$[90/90/0/0]_s$
Plate A1	$[90/90/0/0/d]_s$
Plate B	$[90/0/90/0]_s$
Plate B1	$[90/0/90/0/d]_s$
Plate B2	$[90/0/90/d/0]_s$
Plate B3	$[90/0/d/90/0]_s$
Plate B4	$[90/d/0/90/0]_s$
$E_L$	longitudinal modulus of elasticity
$E_T$	transverse modulus of elasticity
L	length
t	thickness
w	width
$\rho$	density
$\omega$	frequency

## Acronyms

DAQ	Data Acquisition
VI	Virtual Instrument

## Introduction

Conventional structural designs are often unacceptable in coping with modern problems of structural resonance caused by the complex nature of the dynamic environments. Current interest in large flexible space structures provides new motivation and requirements of structural damping enhancement for vibration control. The objective of enhancing damping in structural elements is to control the response of the elements in order to prevent catastrophic failure due to excessive deformation.

In this work, passive damping is used to enhance the damping of a carbon/epoxy cantilever plate under free vibration by adding a viscoelastic-damping layer to the plate. Cantilevered flat plates are convenient simulations for structural components, such as wings, horizontal and vertical stabilizers, and compressor fan blades for aircraft engines.

A number of papers have appeared which explore the effects of interlaminar damping of beam and plate structures. Ditaranto and McGraw [1] investigated the dissipation of vibratory energy in sandwich plates with a viscoelastic core. Only transverse inertial effects were included in the analysis. The solution for the damping was given for simply supported edges, and a relation between modal frequency and loss factor was obtained. Khatua and Cheung [2] used a finite element technique for the study of elastic multi-layer beams and plates. Orthotropy was included in the analysis, but rotatory and translatory inertia effects were neglected. Barrett [3] developed a comprehensive model to predict the damping of composite laminated plates with a viscoelastic layer. The effect of stress coupling and compliant layering was examined. Saravanos and Pereira [4] developed a discrete layer laminate theory for composite laminates with damping layers by incorporating a piecewise continuous displacement field through the thickness. Nadella and Rao [5] applied the modal strain energy method proposed by Johnson and Kienholz [6] to estimate the modal parameters of the multi-damping layer anisotropic laminated composite beams. Gerst, Rao and He [7] presented experimental results for composite beams with single and double damping layers, and demonstrated that cocuring is an effective way of fabricating highly damped composite structural components.

## Objective

In a previous joint research interchange between California Polytechnic State University and NASA-Dryden Research Center entitled, “Hybrid damping system for an electronic equipment mounting shelf”, the ability to detect modes of vibration using surface mounted piezoelectric ceramics (PZT) as sensors was investigated [8]. Resonant frequencies and amplitudes of the damped and undamped plates were determined and presented.

The objective of this study was to investigate the effect of passive damping on composite plates. Five tasks were included in this study: 1) constructing carbon composite plates with different lay-up sequences and staging of the embedded viscoelastic layers, 2) mounting piezoelectric sensors, 3) determining the modal parameters of the plates, 4) numerical analysis utilizing COSMOS/M, and 5) comparison between experimental and numerical analysis.

## Experimental Procedure

The following is a review of the experimental procedure, equipment and materials used in the fabrication and dynamic testing of the cantilever composite plates. Fabrication and testing of these plates were conducted in the Aerospace Composite and Structural Laboratory (ACSL) at California Polytechnic State University.

### Fabrication of Composite Plates

The composite plates were fabricated using carbon fiber/epoxy resin and two layers of viscoelastic material. The passive damping material provides high damping at room temperature but low stiffness and strength. The property of materials used are listed in Tables 1 and 2.

Table 1. Material properties for 977-2 carbon fiber/IM7 epoxy resin.

$E_L$	psi	2.5e7
$E_T$	psi	1.1e6
$\rho$	Lb*s <sup>2</sup> /in <sup>4</sup>	1.43e-4
$\nu$		0.36
t	inches	0.00625

Table 2. Material properties for 3M viscoelastic damping layer, SJ2015 type 1205.

	Degrees F	32-140
E	psi	
$\rho$	Lb*s <sup>2</sup> /in <sup>4</sup>	
$\nu$		0.5
t	inches	0.005

The damped composite plates consist of eight layers of carbon/epoxy and two layers of passive damping material. Several different lay-ups of composite material with and without damping were fabricated. The plate dimension and sequences are listed in Table 3. An example of a typical lay-up is  $[90/0/90/0/d]_s$ , which represents a symmetric lay-up of  $90^\circ$ ,  $0^\circ$ ,  $90^\circ$ ,  $0^\circ$  of composite material and a damping layer,  $d$ , symmetric about the center of the plate as shown in Figure 1.

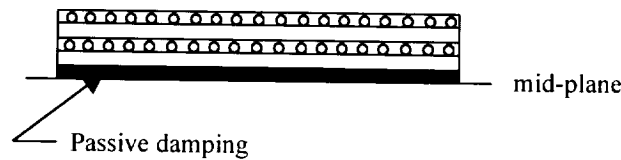


Figure 1. Composite material plate with embedded damping layer.

The lay-ups consisted of 8" x 9" composite plates. The composite lay-up was placed in a composite air press in three steps. The first two steps consisted of curing the top and bottom lay-up of carbon/epoxy with temperature and pressure cycles as recommended by the manufacturer of the prepreg material, separately. The third step was to bond them together with the embedded viscoelastic layers, as recommended by the manufacturer of the 3M material.

Once these plates were fabricated, they were cut into plate samples of 4-in. width and 9-in. length. Two 0.97" x 4" x 0.25" aluminum bars were secured with two bolts sandwiched clamped on one edge of the plate. A third bolt was placed in the center of the aluminum bars, in order to secure the test specimen to the shaking table.

Piezoelectric ceramic sensors (0.75" x 0.5") were bonded with the positive poling axis oriented perpendicular to the top surface. The conductive epoxy allows the surface of the plate to be used as a common negative pole for the sensor. During the bonding process the Air Press applied 80 Lbs force at room temperature for 20 minutes.

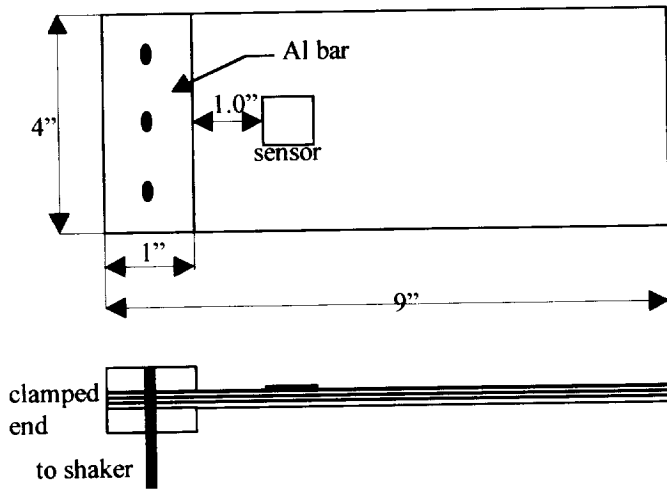


Figure 2. Cantilever Plate

Table 3. Plate dimensions and sequence with and without damping material.

4" x 8" x 0.05"	[90/90/0/0] <sub>s</sub>
4" x 8" x 0.06"	[90/90/0/0/d] <sub>s</sub>
4" x 8" x 0.05"	[90/0/90/0] <sub>s</sub>
4" x 8" x 0.06"	[90/0/90/0/d] <sub>s</sub>
4" x 8" x 0.06"	[90/0/90/d/0] <sub>s</sub>
4" x 8" x 0.06"	[90/0/d/90/0] <sub>s</sub>
4" x 8" x 0.06"	[90/d/0/90/0] <sub>s</sub>

## Identifying Resonant Node Lines

To identify resonant node lines of the test specimen, the carbon fiber plate was mounted on the shaking table and a function generator was used to scan through the frequencies ranging from 0 to 500Hz. Resonant frequencies were identified by sharp rises in audible amplitudes, visual plate displacements, and the formation of node lines using sugar traces on the plate surface.

## Dynamic Testing

A schematic of the experimental setup for dynamic testing of the cantilever plates is presented in Figure 3. A list of the equipment and instrumentation used for testing and fabrication of the plates is given in Table 4.

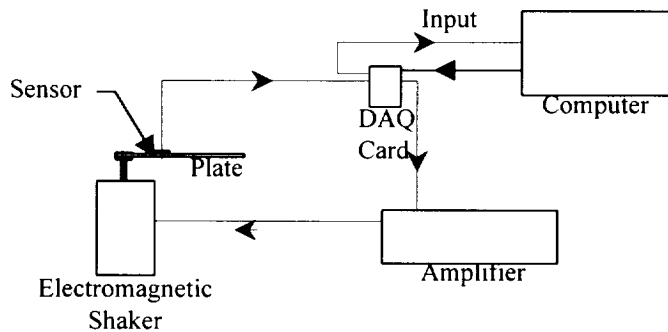


Figure 3. Schematic of Dynamic Testing

Time response and frequency response data was acquired using National Instruments AT-MIO-16F-5 Data Acquisition (DAQ) card in conjunction with National Instruments LabVIEW for Windows Network Analyzer Virtual Instrument (VI). A cantilever plate was mounted on a shaker and excited using a chirp signal from LabVIEW. A power amplifier was used to boost the signal before entering the shaker. The DAQ card acquires the data signals directly from the sensor, conditions and digitizes the data, and enters the data into the PC's bus.

Table 4. Equipment and Instrumentation Summary

MB Electronics		
Hewlett-Packard	3311A	EE-3955
		8" x 9" plate
Morgan Matroc Inc.	PZT-5A	l = 0.75 w = 0.5 t = 0.01
Thurston	H.S.S.	d = 1.74" t = 0.06"
Witco	AT2000	486-66DX2
National Instruments	Version 3.1	DAQ Software: Network Analyzer
National Instruments	AT-MIO-16F-5	max. input: $\pm 10$ volts max. sample rate: 51.2K
Tektron	7912	2 Channel
Kistler	5122	4 Channel

### Chirp Signal Tests

The chirp signal is an impulsive type of signal that can have excitation over a wide range of frequencies, and avoids impulse loading problems. The Network Analyzer provided the chirp signal for the shaking table and sampled the data provided by the sensors. The following Network analyzer parameters were used for the chirp tests:

- 1) Sample rate                      1,000 samples/sec
- 2) Frame size                        1,024 samples
- 3) Windowing                        Hann
- 4) Averaging                         3

Each test included the following steps:

- 1) initiating chirp noise,
- 2) sampling of data provided by sensors,
- 3) recording resonant frequencies represented by relative maximums,
- 4) saving frequency and amplitude data into a spreadsheet file for comparison of with subsequent results.

## Results and Discussion

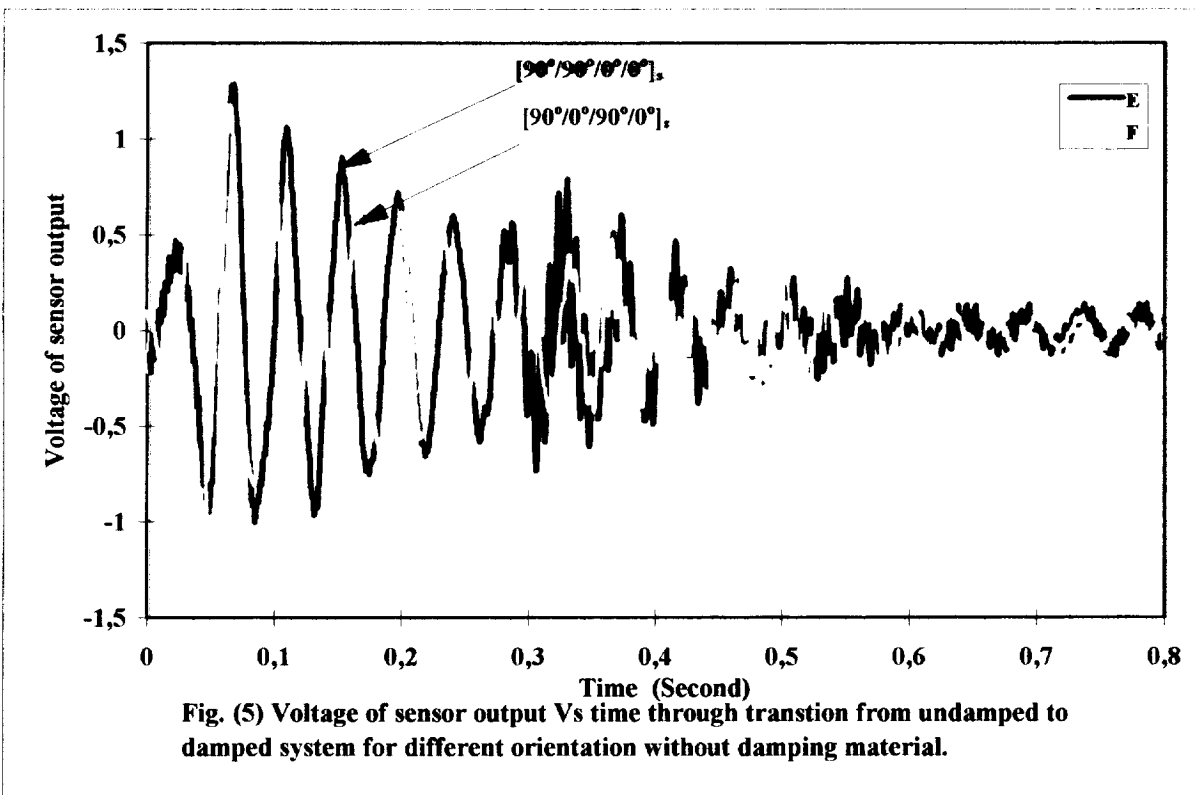
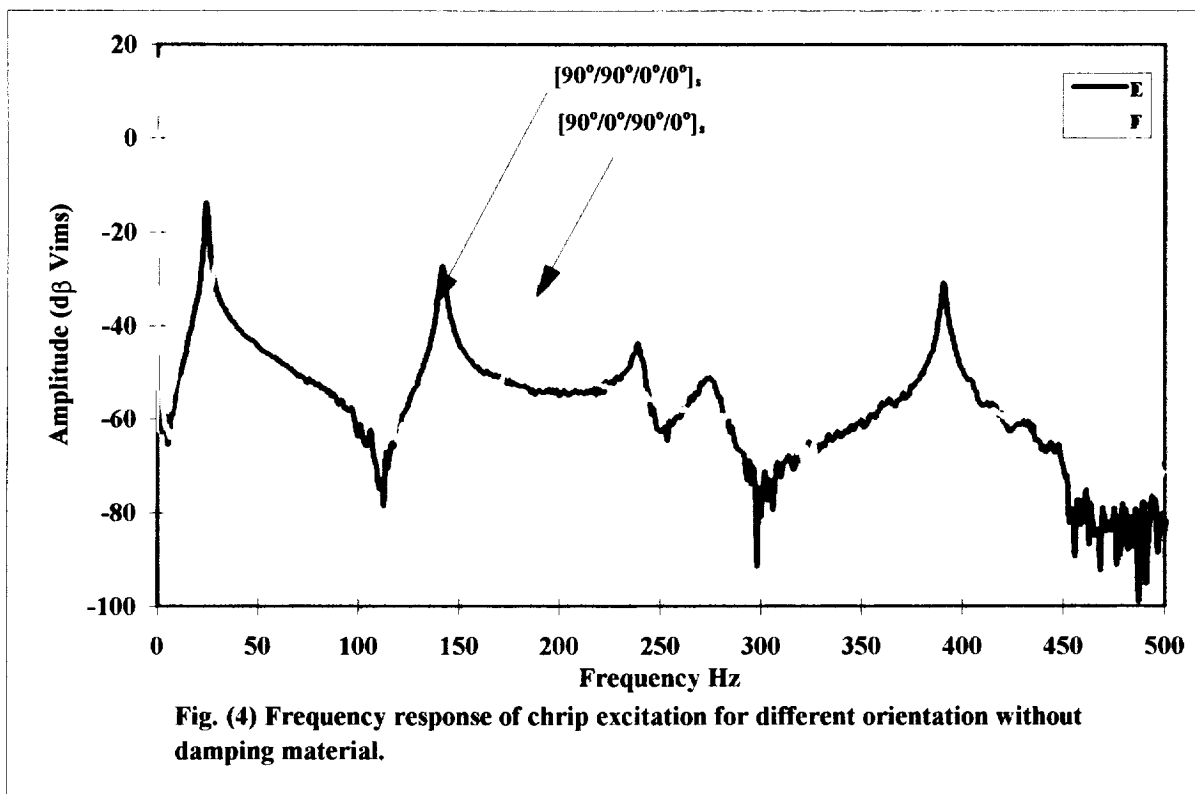
### Experimental Results

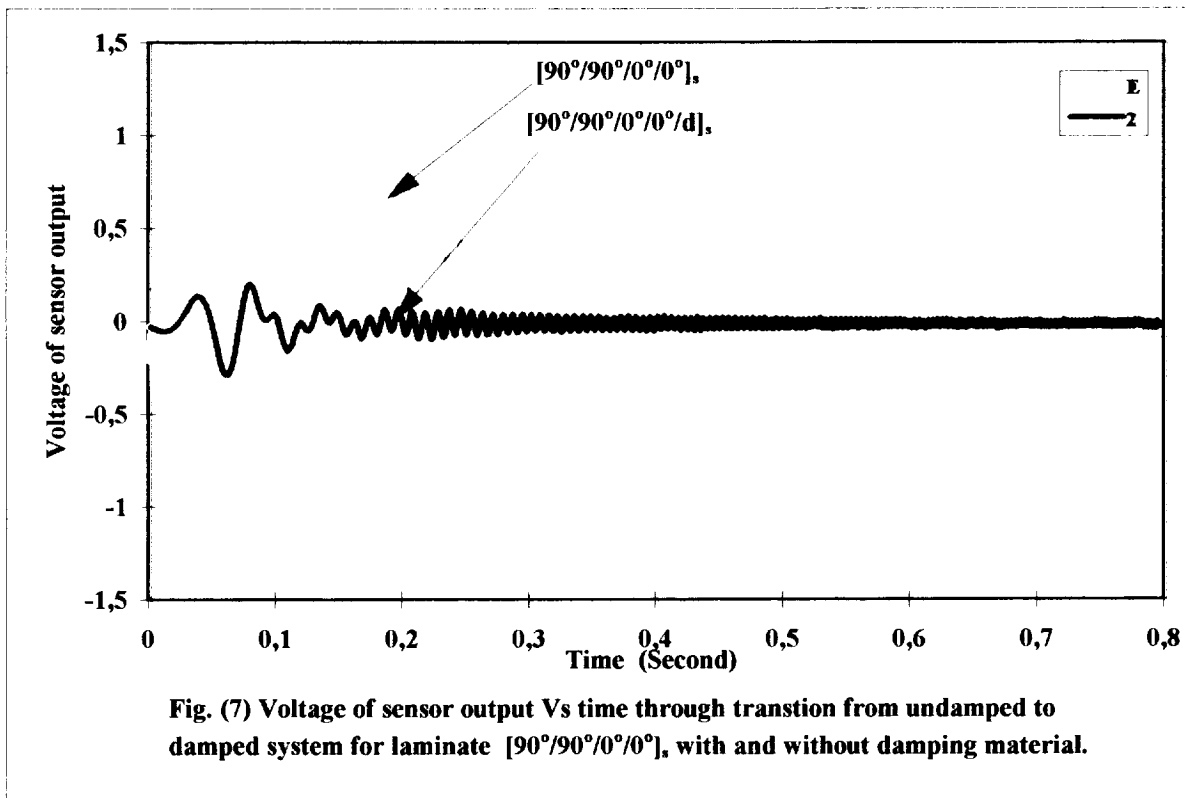
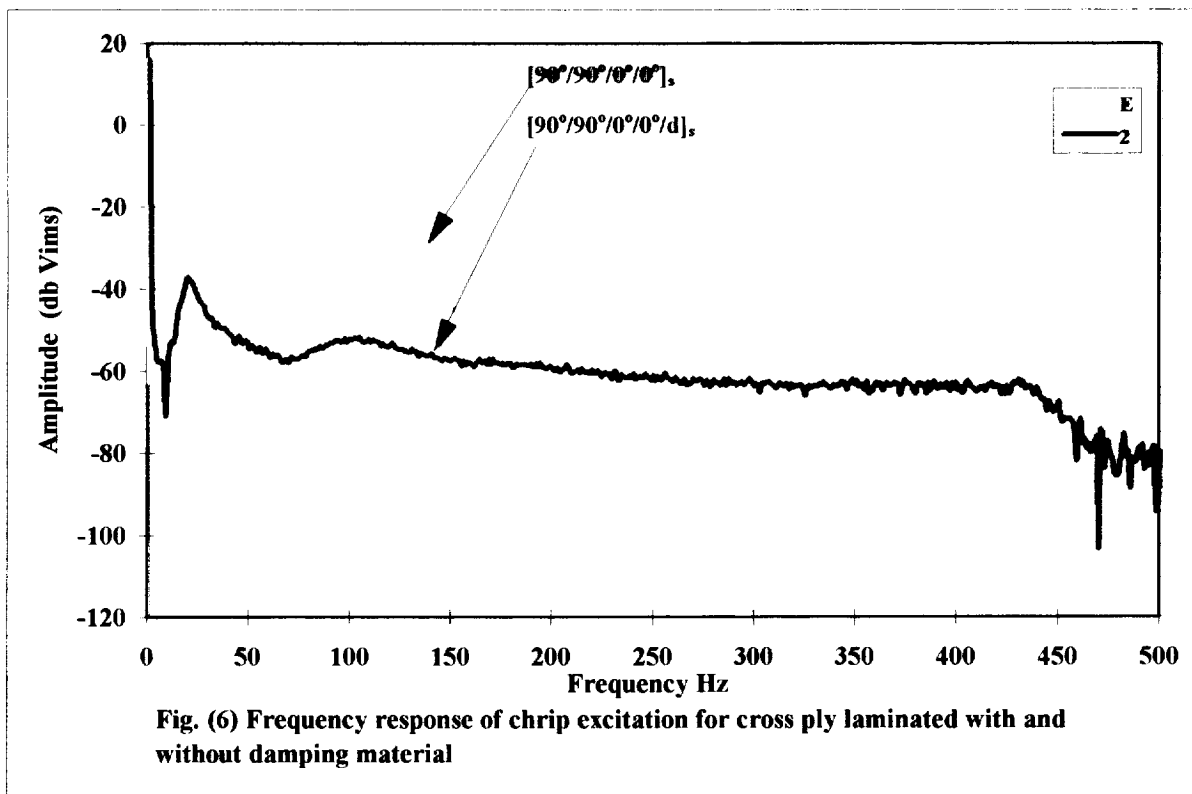
Figure 4 and 5 show the free vibration frequency response and time response curves for plates A and B without damping,  $[90/90/0/0]_s$  and  $[90/0/90/0]_s$ , respectively. For the first mode, these figures show that the change in orientation has no significant effect on the natural frequencies and amplitudes. For the second and third modes of plates A and B, the orientations of the plates have a significant effect on amplitude and natural frequencies. The change in orientation has little effect on the time response. Figure 6 shows the frequency response curves for plates A and A1,  $[90/90/0/0]_s$  and  $[90/90/0/0/d]_s$ , respectively. Plate A1,  $[90/90/0/0/d]_s$ , has two damping layers located about the mid-plane of the plate. One can see that the second and third modes are completely damped out, and the first resonant frequency and amplitude decreased with the addition of damping layers. Figure 7 presents the free vibration time response curves for plates A and A1. As can be seen from this figure, the embedded damping layer has a significant effect on the sensor output voltage of the time response curves. Plate A reached steady state at about 0.55 sec., whereas by adding the damping layer, the steady-state time response was reached in 0.15 sec.

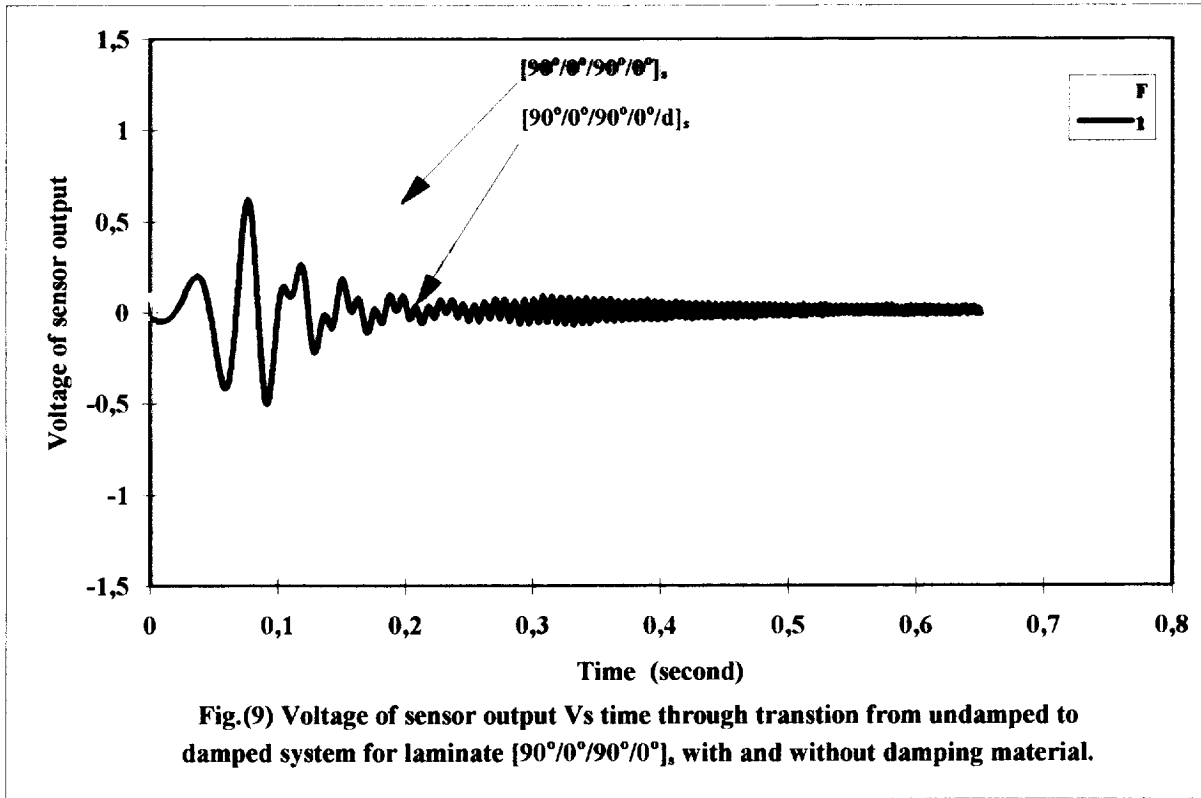
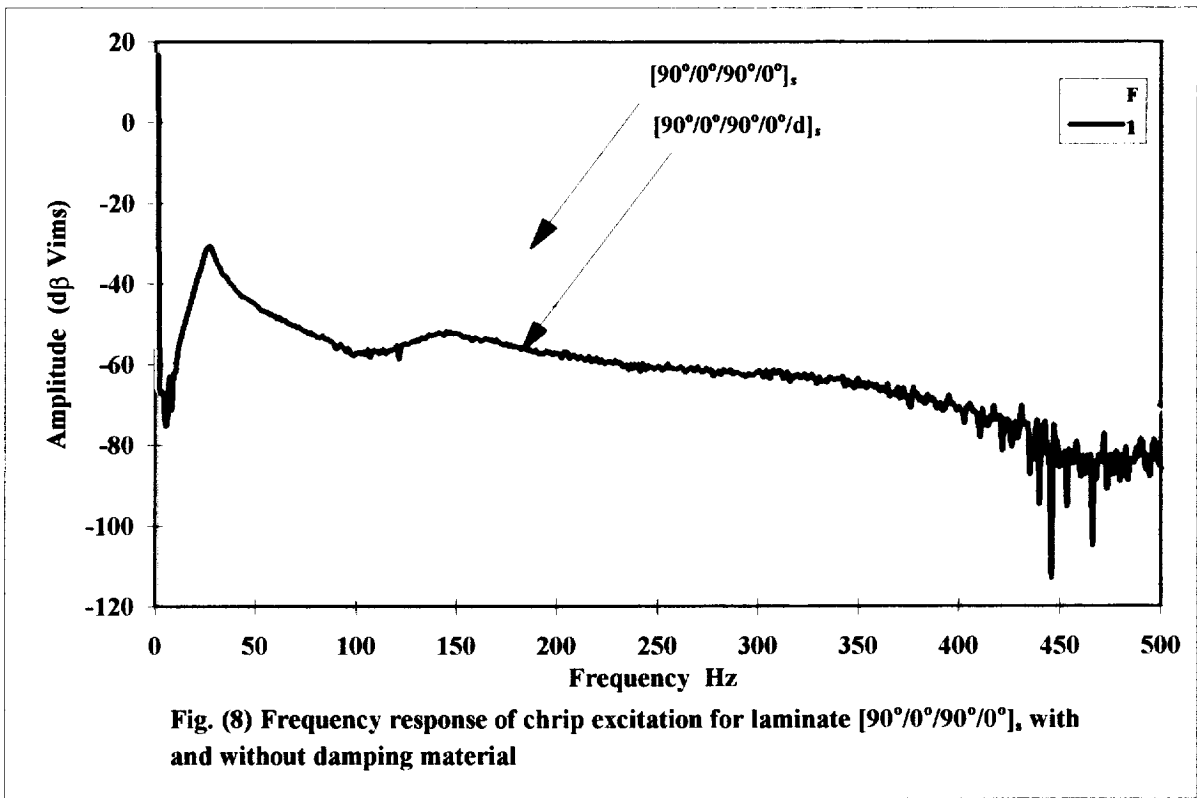
Figures 8 and 9 present the free vibration frequency response curves and the time response curves for plates B and B1,  $[90/0/90/0]_s$  and  $[90/0/90/0/d]_s$ , respectively. The decrease in frequency and the increase in damping can be seen in both figures. To reduce the frequency response, the damping material is more effective at higher modes rather than the lower modes.

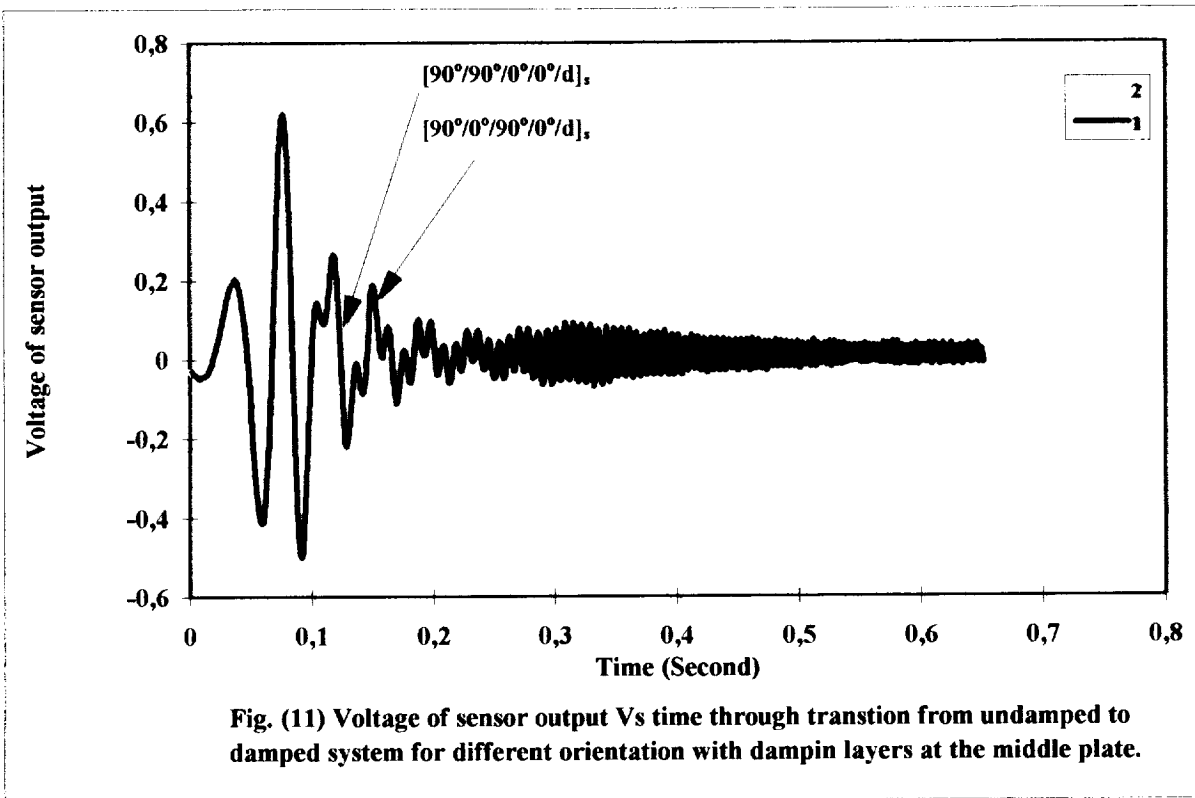
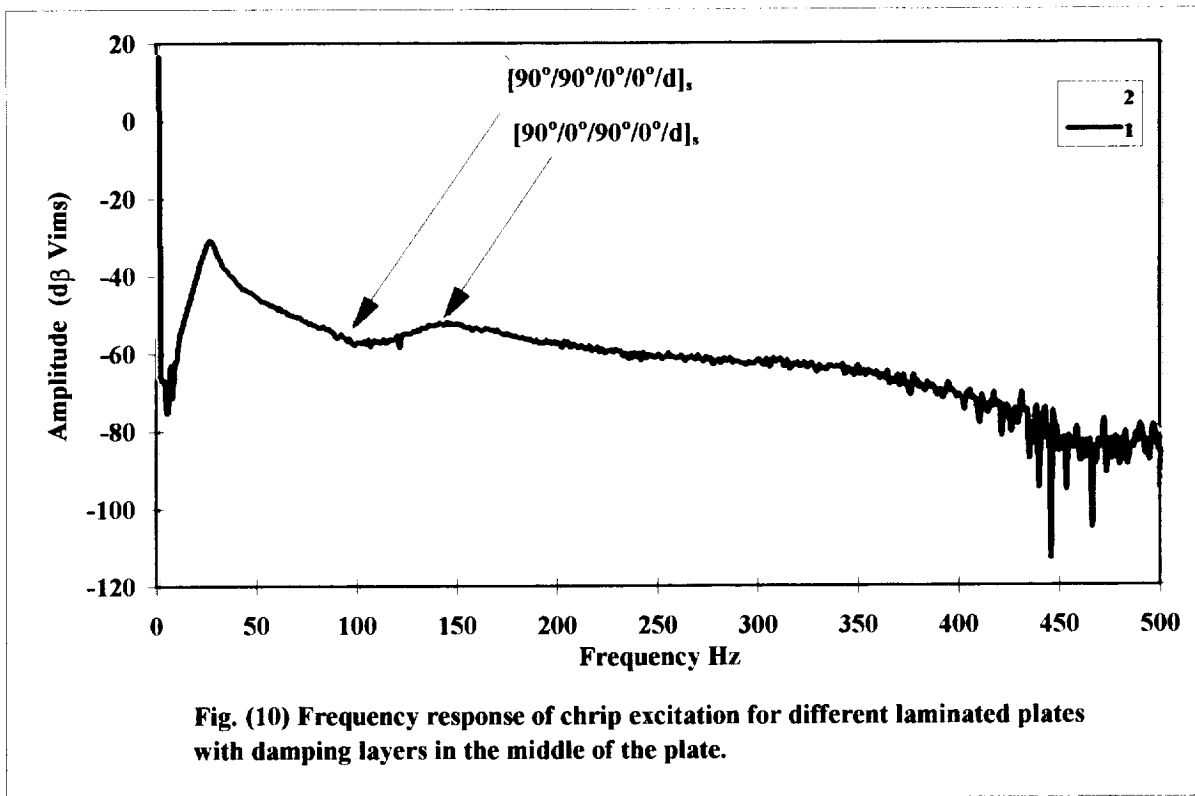
Figures 10 and 11 show the effects of adding two damping layers about the mid-plane to plates with different orientations,  $[90/90/0/0/d]_s$  and  $[90/0/90/0/d]_s$ . The resonant frequencies for the  $[90/0/90/0/d]_s$  plate appear to be much higher than the  $[90/90/0/0/d]_s$  plate. This is due to the change in the orientation of the lay up, making the  $[90/0/90/0/d]_s$  plate stiffer than the  $[90/90/0/0/d]_s$  plate. Also, there is a significant change in amplitude and time response curve for the  $[90/0/90/0/d]_s$  plate.

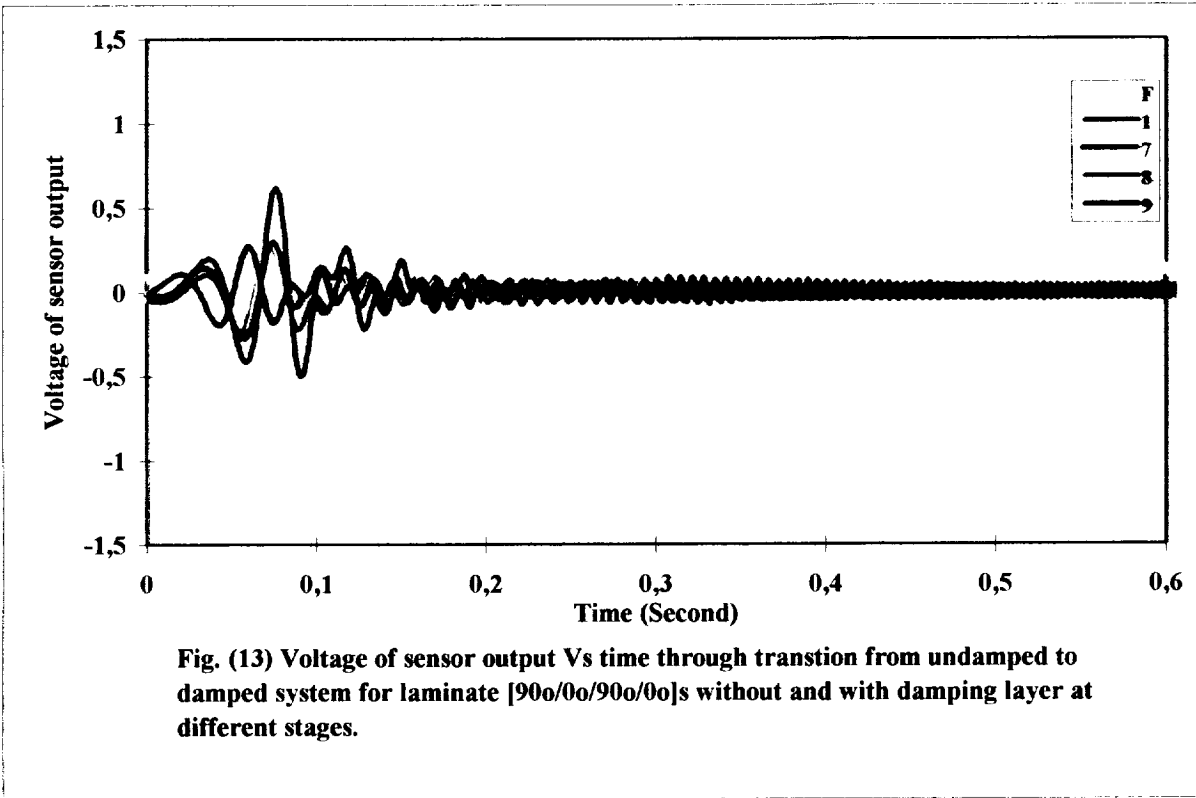
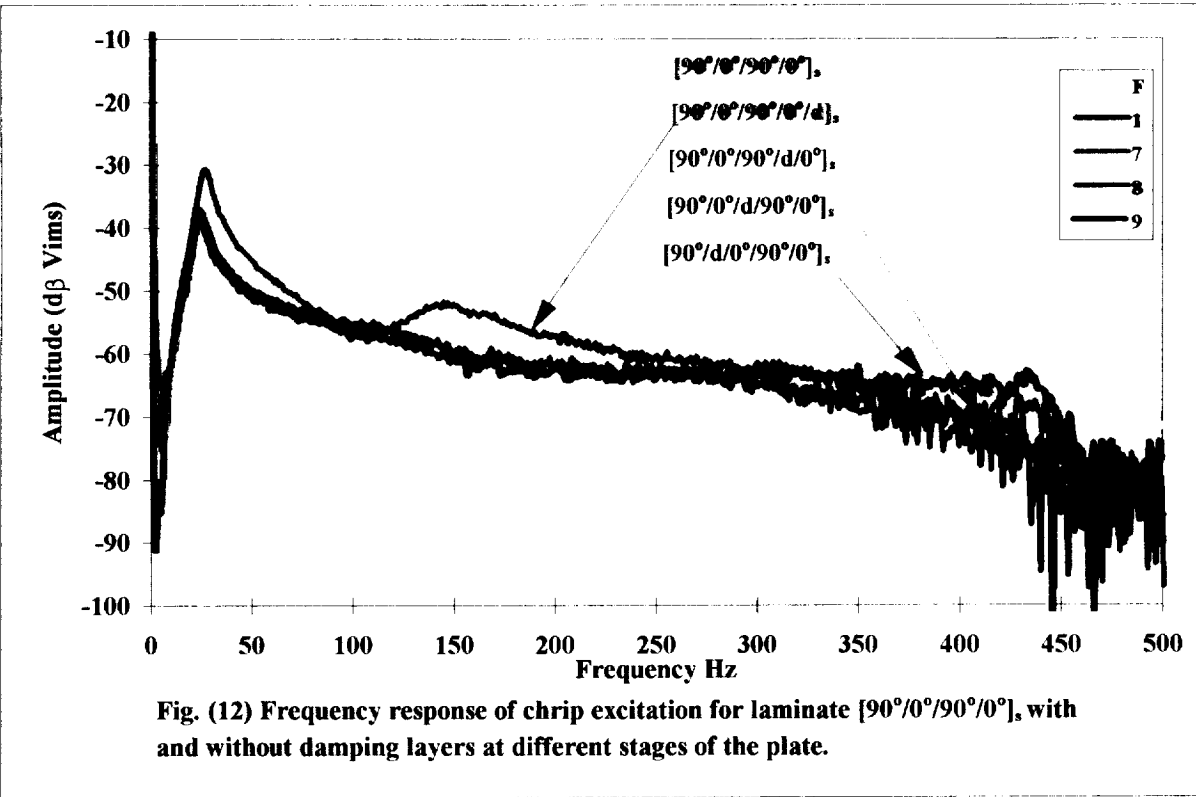
Figures 12 and 13 present the frequency response and time response curves for plates with and without damping for sequence  $[90/0/90/0]_s$ . The damping layers are embedded at different locations. The closer the embedded layer is to the surface, the











higher the damping of the plate. The plate with the embedded viscoelastic layer at the mid-plane, plate B1, is the least effective for damping. Regardless of location, the embedded viscoelastic layers significantly enhances the damping of the plates.

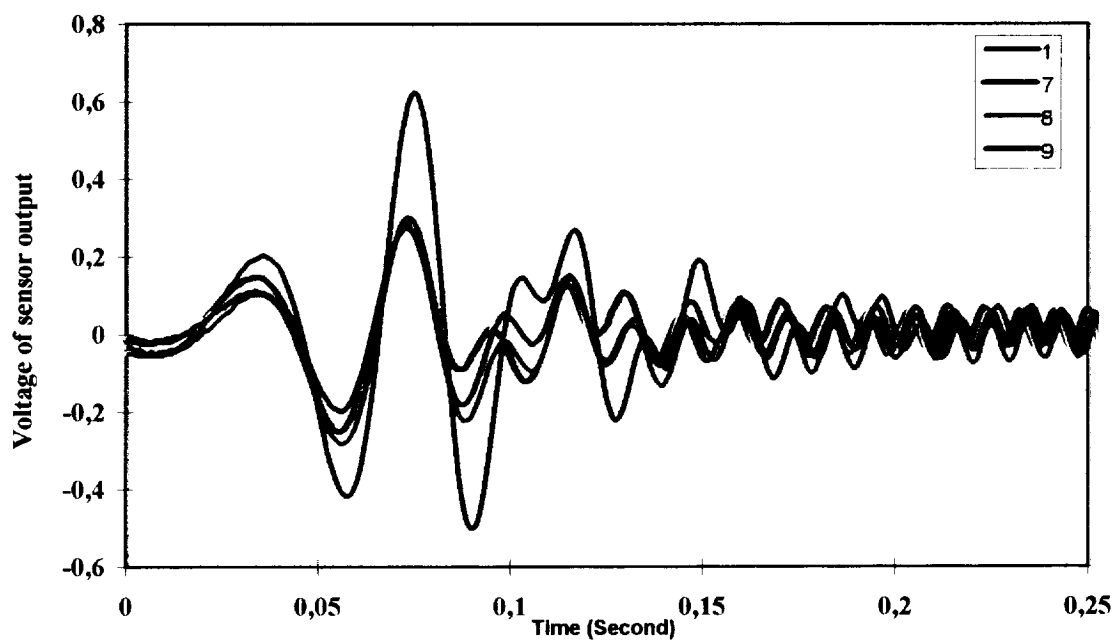
Whenever the plate is subjected to cyclic bending, the composite constraining layers will constrain the viscoelastic material and force it to deform in shear, which is how the vibrational energy is dissipated. This is why the plates with embedded viscoelastic layers show an increase in damping. The obvious decrease in natural frequencies of the plates with damping is caused by the decrease in stiffness introduced with the addition of the damping layers.

Figure 14 shows the time response curves for plates with damping for orientation  $[90/0/90/0]_s$ , plates B1 through B4; the damping layers are embedded at different locations. Plate B1 is the least effective for damping. One can see that the shear damping is clearly a function of constraining layer thickness. The variation of the damping amplitude is due to the change in location of the embedded damping layer within the plates.

Table 5 lists the natural frequencies obtained from the chirp tests for the first three bending modes for all plates.

Table 5. Frequency modes for different orientations with and without embedded layers.

$[90/90/0/0]_s$	22.46	140.62	388.67
$[90/90/0/0/d]_s$	19.53	98.63	--
$[90/0/90/0]_s$	30.27	186.52	486.3
$[90/0/90/0/d]_s$	25.39	142.57	--
$[90/0/90/d/0]_s$	20.51	--	--
$[90/0/d/90/0]_s$	23.44	--	--
$[90/d/0/90/0]_s$	23.44	--	--



**Fig. (14) Voltage of sensor output Vs time through transtion from undamped to damped system for laminate [90/0/90/0]s with damping layer at different stages.**

## Numerical Results

COSMOS/M version 1.75 finite element analysis software was used to verify the experimental results for plates A and B. The finite element model (FEM) and the mode shapes for plates A and B are shown in Figures 15 and 16. The FEM consists of a total of 200 elements. The element stiffness matrix was formulated using QUAD4 technique. Small deflections and linear elastic properties were assumed. The subspace iteration method was used for the frequency analysis.

Table 6 presents the numerical and experimental resonant frequencies for plates A and B, without damping. The first and second modes are in good agreement for both plates. Because the higher modes are dependent on the lower modes for the numerical analysis, the third mode significantly differs from the experimental values obtained for both plates.

Table 6. Numerical and experimental resonant frequencies for plates without damping.

	Num.	Exp.	Num.	Exp.	Num.	Exp.
	21.39	22.46	133.87	140.62	375.49	237.30
	30.95	30.27	193.84	186.52	543.37	375

Figure 15. Finite Element Model and Mode Shapes of Plate A [90/90/0/0]s

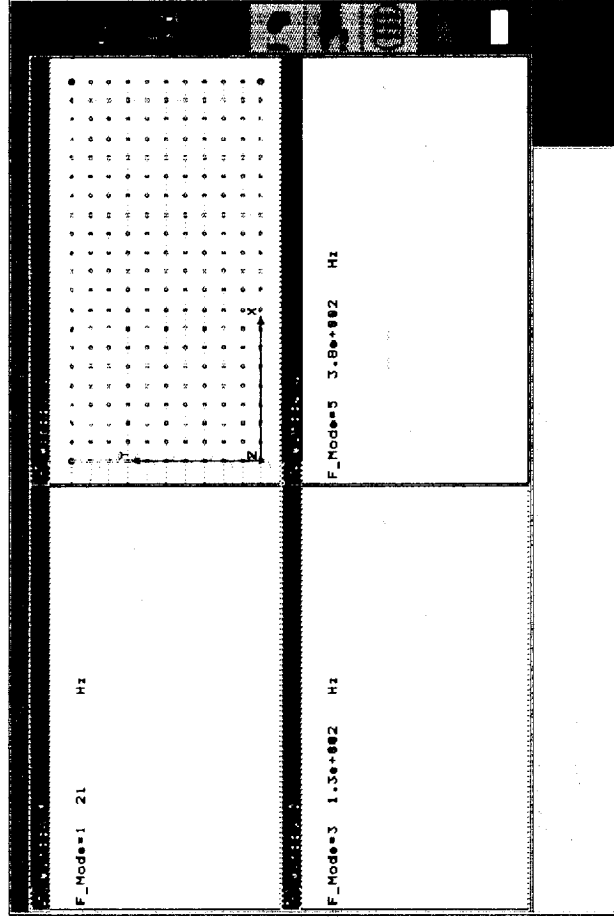
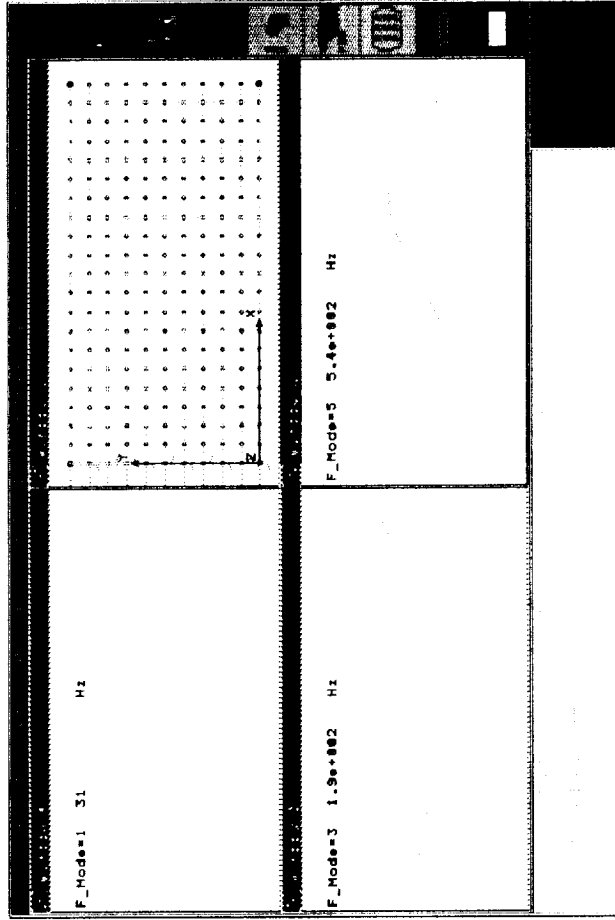


Figure 16. Finite Element Model and Mode Shapes of Plate B [90/0/90/0]s



## CONCLUSION

This study has shown an effective way of damping composite structure components and different laminated structures, which have wide applications where vibration and noise reduction are of main concern. The addition of the damping layer (3M) material increased the damping ratio and decreased the stiffness/mass ratio. Careful selection of embedded damping layer location and laminate orientation are necessary to optimize the damping benefits desirable and stiffness reductions that can be tolerated. The addition of viscoelastic material in plate B1,  $[90/0/90/0]_s$ , further reduces the amplitude of vibration in all the fundamental bending mode frequencies more effectively than plate A1,  $[90/90/0/0/d]_s$ . This is because the stiffness/mass ratio for the first plate is greater than that for the second plate. Excellent agreement between numerical and experimental results for plates without damping was obtained for the natural frequencies of the system.

## REFERENCES

- [1] Ditaranto, R. A., and J. R. McGraw, Jr., 1969. Vibratory bending of damped laminated plates. *Journal of Engineering for Industry* 91,1081-1090.
- [2] Khatua, T. P., and Y. K. Cheung, 1973. Bending and vibration of multilayer sandwich beams and plates. *International Journal of Numerical Methods for Engineers* 6(1), 11-24.
- [3] Barrett, D. J., 1992. An anisotropic laminated damped plate theory. *Journal of Sound and Vibration* 154(3), 453-465.
- [4] Saravanos, D. A., and J. M. Pereira, 1992. Effects of interply damping layers on the dynamic characteristics of composite plates. *AIAA Journal* 30(12), 2906-2913.
- [5] Nadella, Satish, and Mohan D. Rao, 1995. Damping of composite structures using embedded viscoelastic layers. *Proceedings of the 13<sup>th</sup> International Modal Analysis Conference, Nashville, Tennessee* V1, 233-239.
- [6] Johnson, Conor D., and David A. Kienholz, 1981. Finite element prediction of damping in structures with constrained viscoelastic elements. *AIAA Journal* 20(9), 1284-1290.
- [7] Gerst, D., M. D. Rao, and S. He, 1992. Damping of co-cured composite structures incorporating viscoelastic materials. *Proceedings of the Damping of Multiphase Inorganic Materials Symposium*, 85-93, Chicago, Illinois, 2-5 November 1992.
- [8] J. R. Cavalli, E. I. Elghandour and F. A. Kolkailah, 1997. Hybrid damping system for an electronic equipment mounting shelf. NASA-Ames Research Center, Ca, NCA2-779, 1997.